

**Electron compound nature in a surface atomic layer of a two-dimensional hexagonal lattice**

Iwao Matsuda,<sup>1,\*</sup> Fumitaka Nakamura,<sup>1</sup> Keisuke Kubo,<sup>2</sup> Toru Hirahara,<sup>2</sup> Shiro Yamazaki,<sup>1</sup> Won Hoon Choi,<sup>3</sup> Han Woong Yeom,<sup>3</sup> Hisashi Narita,<sup>1</sup> Yuki Fukaya,<sup>4</sup> Mie Hashimoto,<sup>4</sup> Atsuo Kawasuso,<sup>4</sup> Masanori Ono,<sup>1</sup> Yukio Hasegawa,<sup>1</sup> Shuji Hasegawa,<sup>2</sup> and Katsuyoshi Kobayashi<sup>5</sup>

<sup>1</sup>*Institute for Solid State Physics, The University of Tokyo, Kashiwa 277-8581, Japan*

<sup>2</sup>*Department of Physics, The University of Tokyo, 7-3-1 Hongo, Bunkyo-ku, Tokyo 114-0033, Japan*

<sup>3</sup>*Department of Physics and Center for Atomic Wires and Layers, POSTECH, Pohang 790-784, Korea*

<sup>4</sup>*Advanced Science Research Center, Japan Atomic Energy Agency, 1233 Watanuki, Takasaki, Gunma 370-0033, Japan*

<sup>5</sup>*Department of Physics, Faculty of Science, Ochanomizu University, 2-1-1 Otsuka, Bunkyo-ku, Tokyo 112-8610, Japan*

(Received 14 August 2010; published 25 October 2010)

The two-dimensional (2D) ordered phase of monovalent metal alloy,  $\sqrt{21} \times \sqrt{21}$ , is formed on the Si(111) surface with the constant electron/atom ratio, indicating electron compound nature. Two conventional theories of the Hume-Rothery compounds, Jones model (nearly-free-electron model), and pseudopotential model (interionic interaction model), were applied to examine stability of the 2D phase. We found breakdown of the former and confirmation of the latter approaches with importance of medium-range interatomic interaction, mediated by the 2D surface-state electrons, in the latter approach.

DOI: [10.1103/PhysRevB.82.165330](https://doi.org/10.1103/PhysRevB.82.165330)

PACS number(s): 73.20.At, 68.35.-p, 73.61.At, 79.60.Dp

**I. INTRODUCTION**

Among numerous numbers of metallic materials, being composed of various combinations of elements, there is a tendency in metal alloys for definite crystal structures to form at characteristic electron concentrations.<sup>1</sup> Electron concentration has conventionally been expressed as the ratio of all conduction electrons to the number of atoms,  $e/a$ . This factor has been of particular prominence in the large group of alloy phases based on three noble metals, Cu, Ag, and Au, and has led to establishment of the Hume-Rothery rule,<sup>2,3</sup> a strong correlation between the  $e/a$  ratio and the adopted crystal structure. Based on this experimental rule, stability of such alloys, so-called electron phases or electron compounds, has been argued in terms of a relation between the Fermi surface (FS) ( $e/a$ ) and the Brillouin zone (BZ) (the crystal structure).<sup>2,3</sup>

While such researches have been performed for bulk metal alloys with three-dimensional (3D) Fermi surfaces and 3D crystal structures,<sup>2,3</sup> there has been little report on electron compounds in low-dimensional systems despite the appearance of specific phenomena that can provide distinct insights to this issue. Among numerous numbers of 2D ordered phases of metal alloys reported on crystal surfaces, we notice that  $\sqrt{21} \times \sqrt{21}$  ordered phases, prepared by coadsorptions of various noble and alkali-metal atoms on the Si(111) substrate, form at constant  $e/a$  ratio in spite of the differences in the chemical compositions, local atomic structures, and the surface preparation procedures.<sup>4-16</sup> As listed in Table I, the conduction-electron number in the unit cell and the total metal coverage are always three electrons and 1.1–1.2 monolayer (ML), respectively, meaning a constant  $e/a$  ratio.

In the present research, we show the further evidence of a close relation between the  $e/a$  and the  $\sqrt{21} \times \sqrt{21}$  surface superstructure. Then, we examine stability of this 2D phase by applying the two conventional theories for the Hume-Rothery phases, Jones model [nearly-free-electron (NFE) model], and pseudopotential model (conduction-electron-

mediated interionic interaction model).<sup>1-3</sup> Natures of the 2D electron compound are explained in terms of the pseudopotential approach with the critical role of medium-range 2D interatomic interaction, mediated by the 2D surface-state electrons.

**II. EXPERIMENTAL**

A distinct  $\sqrt{21} \times \sqrt{21}$  phase was found through observations by reflection high-energy electron (positron) diffraction, RHEED (RHEPD), and scanning tunneling microscopes, STM, as shown in Figs. 1(a)–1(d). The surface was formed by the 0.7 ML-Ag deposition at 450 °C on a periodic array of one-dimensional Au atomic chains, a Si(111)5 × 2-Au surface,<sup>17,18</sup> prepared by the 0.4–0.5 ML-Au deposition on Si(111)7 × 7. The RHEPD experiments were carried out in a UHV chamber equipped with a positron source of <sup>22</sup>Na and electromagnetic lens system.<sup>8</sup> The RHEPD pattern was obtained at room temperature with the incident positron beam of 10 kV. The STM observation was performed at room temperature and the instrumental details were described elsewhere.<sup>5-7</sup> The Ag coverage was determined by Ag 3d core-level photoemission spectroscopy measurement at  $h\nu=500$  eV with synchrotron radiation at beamline BL-8A1 at Pohang Light Source in Korea. Electronic bands (Fermi surfaces) were measured by angle-resolved photoemission spectroscopy with the He I $\alpha$  radiation.<sup>4</sup> In the present research, scanning tunneling spectroscopy (STS) observation<sup>19</sup> was also performed at 5 K on the 2D Ag nanocluster<sup>5,20</sup> on Si(111) $\sqrt{3} \times \sqrt{3}$ -Ag for the discussion described below.

**III. RESULTS AND DISCUSSION**

Figures 1(c) and 1(d) show empty- and filled-state STM images of the surface taken at room temperature, respectively. The STM features were similar to previous reports of  $\sqrt{21} \times \sqrt{21}$  phases prepared by Ag or Au adsorption on

TABLE I. Examples of the reported preparation procedures for the metal-induced  $\sqrt{21} \times \sqrt{21}$  phases on Si(111). Initial phases, Phase<sup>in</sup>, and adatoms, Ad, are indicated with coverage ( $\theta^{\text{Phase}}$ ,  $\theta^{\text{Ad}}$ ). Total metal coverage  $\theta^{\text{total}}$ , and a number of valence electrons per  $\sqrt{21} \times \sqrt{21}$  unit cell,  $n^{\text{val}}$ , are listed. 1 ML (monolayer) corresponds to the Si(111) surface atomic density,  $7.8 \times 10^{14}$  atoms/cm<sup>2</sup>.

Phase <sup>in</sup> ( $\theta^{\text{Phase}}$ )	Ad ( $\theta^{\text{Ad}}$ )	$\theta^{\text{total}}$ (ML)	$n^{\text{val}}$	Ref.
$\sqrt{3} \times \sqrt{3}$ -Ag (1.0 ML)	Na (0.1–0.2 ML)	1.1–1.2	3	4, 7, and 16
$\sqrt{3} \times \sqrt{3}$ -Ag (1.0 ML)	K (0.1–0.2 ML)	1.1–1.2	3	14
$\sqrt{3} \times \sqrt{3}$ -Ag (1.0 ML)	Cs (0.1–0.2 ML)	1.1–1.2	3	6 and 14
$\sqrt{3} \times \sqrt{3}$ -Ag (1.0 ML)	Ag (0.1–0.2 ML)	1.1–1.2	3	4 and 13
$\sqrt{3} \times \sqrt{3}$ -Ag (1.0 ML)	Au (0.1–0.2 ML)	1.1–1.2	3	5, 8, 9, and 15
$\sqrt{3} \times \sqrt{3}$ -Au ( $\sim 0.9$ ML)	Ag (0.2–0.3 ML)	1.1–1.2	3	11 and 12
$5 \times 2$ -Au (0.4–0.5 ML)	Ag ( $\sim 0.7$ ML)	1.1–1.2	3	This study

Si(111) $\sqrt{3} \times \sqrt{3}$ -Ag.<sup>4,5,9,21</sup> Our RHEPD rocking intensity analysis also supported a close structural similarity among the Si(111) $\sqrt{21} \times \sqrt{21}$ -(Au,Ag) surfaces.<sup>22</sup> Due to existence of total reflection angle region for a positron beam, the probing depth is less than 2 Å and RHEPD is the most surface-sensitive diffraction technique.<sup>23,24</sup> These experimental results of the surface structure analyses indicates that the noble-metal  $\sqrt{21} \times \sqrt{21}$  phases have the same atomic structure despite different Ag/Au ratios.

Let us now move on to the electronic structure. Figure 2 shows results of Fermi surfaces and bands mapped by angle-resolved photoemission spectroscopy. The Si(111) $\sqrt{21} \times \sqrt{21}$ -(Au,Ag) surface is an isotropic 2D metal and has a Fermi circle at  $\bar{\Gamma}$  point with the Fermi vector,  $k_F$ , of 0.24 Å<sup>-1</sup>. Since area of the surface BZ (SBZ) corresponds to two electrons in a unit cell, the area ratio between the Fermi circle and the  $\sqrt{21} \times \sqrt{21}$  SBZ indicates that the conducting band is filled with three electrons in a unit cell. The bottom of the parabolic band at  $\bar{\Gamma}'$  (not shown) has an effective mass,  $m^*/m_0$ , of 0.42, where  $m_0$  is the electron mass. The system has energy gaps of  $\sim 150$  meV at 0.2–0.3 eV away from  $E_F$  at the zone boundaries as shown in Figs. 2(a)–2(d). Similar band structures have been reported for other  $\sqrt{21} \times \sqrt{21}$  phases with different Ag/Au ratios,<sup>4,13,14</sup> listed in Table I, and they have been reproduced by the first-principles band calculations.<sup>13,16</sup>

As described above, Table I indicates a universal relation of the  $\sqrt{21} \times \sqrt{21}$  periodicity and the  $e/a$  ratio. The property reminds the Hume-Rothery compounds<sup>2,3</sup> and it is likely characterized in the same way. Early theories for stability of electron compounds have been based on the density of states (DOS) and mainly formulated by Jones.<sup>2</sup> In the well-known NFE model, free-electron spheres allocated in each BZ as centered on the  $\bar{\Gamma}$  points, electron bands form energy gaps at the zone boundaries when the band crosses with their neighbors through band hybridizations. However, there are always remnant DOS at  $E_F$ , a partial gap since overlaps of free-electron spheres and BZ are imperfect in 3D crystals and energy position of the gaps are different among the zone boundaries. When such partial gaps are formed at  $E_F$ , metal alloys are stabilized by reduction in electrons at the highest energy ( $E_F$ ). This graphical relation between Fermi surface

and Brillouin zone is called the FS-BZ effect. Thus, an  $e/a$  ratio directly defines a crystal structure. In this model, the amount of DOS reduction in partial gap at  $E_F$  is crucial in understanding the stability of metal alloys.<sup>2,3</sup>

Stability of the electron compound is described by the FS-BZ effect and it is widely calculated by the Jones model,<sup>2,3</sup>

$$\Delta E = \int_0^{E_{F2}} E \cdot D^{\text{NFE}}(E) dE - \int_0^{E_{F1}} E \cdot D^{\text{FE}}(E) dE, \quad (1)$$

where  $D^{\text{FE}}(E) = m^*/\pi\hbar^2$  and  $D^{\text{NFE}}(E)$  are DOS of FE model and NFE model, respectively.  $E_{F1}$  and  $E_{F2}$  are Fermi energy, referred from the band bottom, of the FE and NFE models, respectively. This equation indicates that the stability is described in terms of the DOS change by a formation of a new periodicity. Therefore, we have conducted the numerical DOS calculation for the NFE model in the 2D hexagonal lattice with band parameters reproducing the experimental band structure (Fermi surface) in Fig. 2. As shown in Fig. 3(a),  $D^{\text{NFE}}(E)$  contains an energy gap, not a partial gap, and a system becomes insulating with two electrons in a unit cell. It is noted that existence of the insulating phase is sharply distinctive from the FE system, being metallic with any number of electrons, and also from the typical 3D Hume-Rothery metal alloys, leaving remnant DOS (a partial gap). Inserting  $D^{\text{FE}}(E)$  and  $D^{\text{NFE}}(E)$  in the above equation, the energy difference,  $\Delta E$ , was calculated with different number of electrons, as summarized in Fig. 3(b). This result indicates that, in Jones model, the hexagonal electronic system is the most stable when it is insulating and filled with two electrons per cell. This is contrast to the band filling of three electrons per cell measured by the photoemission experiment (Fig. 2), indicating a failure of the Jones model in the present 2D system.

It is worth mentioning that the  $\sqrt{21} \times \sqrt{21}$  phase has a 2D NFE system with the energy splitting close to the Fermi level. Thus, a conventional formula of the FE model,

$$k_F^{\text{FE}} = \sqrt{2\pi n_{2D}} \quad (2)$$

is no longer appropriate to precisely determine 2D electron density,  $n_{2D}$ , from the Fermi wave vector,  $k_F^{\text{FE}}$ . On the other hand, the present DOS calculation on two-dimensional hex-

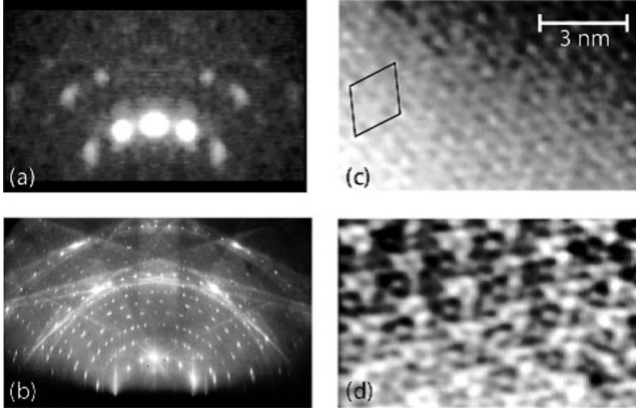


FIG. 1. (a) RHEPD and (b) RHEED patterns of  $\sqrt{21} \times \sqrt{21}$  phase prepared by 0.7 ML-Ag deposition on Si(111)5 $\times$ 2-Au at 450 °C. The RHEPD spots are much diffusive than the RHEED one due to strong surface sensitivity (Ref. 24) (c) filled (+1.0 V) and (d) empty-state (-1.5 V) STM images of the  $\sqrt{21} \times \sqrt{21}$  phase with a schematic  $\sqrt{21} \times \sqrt{21}$  unit cell.

agonal lattice has demonstrated clear distinction of electronic structure between insulating and metallicity at two and three electrons in the unit cell, respectively. Observation of the clear Fermi surfaces with the Fermi wave vector close to  $k_F^{\text{FE}}$  with three electrons per cell definitely indicates that the  $\sqrt{21} \times \sqrt{21}$  phase has three valence electrons in the unit cell.<sup>4,14,15</sup>

In another approach of the structure stabilization, a framework of the pseudopotential theory has been adopted by Heine, Weaire, and Blandin in understanding the stability of the electron compounds.<sup>2,3</sup> Through the second perturbation calculation of the individual ion pseudopotentials, they found the significant contribution of the band-structure energy,  $E_{bs}$ , that depends on the local position of atoms.<sup>2,3</sup> This expression can be written exactly by a sum of pair interactions,  $V(r_{ij})$ , between atoms,

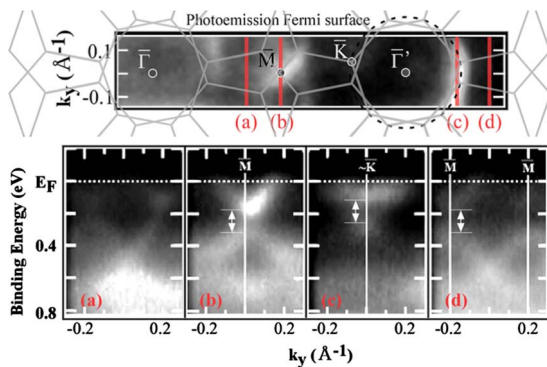


FIG. 2. (Color online) Fermi-surface map of the Si(111) $\sqrt{21} \times \sqrt{21}$ -(Au, Ag) surface in Fig. 1 with SBZ of the two domains. The measurement was by taking photoemission intensity at Fermi level with He I $\alpha$  source at room temperature. (a)–(d) Grayscale energy diagram along wave vectors,  $k_y$ , indicated as thick (red) line at the alphabet in the figure. Energy gaps and a free-electron circle are indicated by arrows and a broken line, respectively.

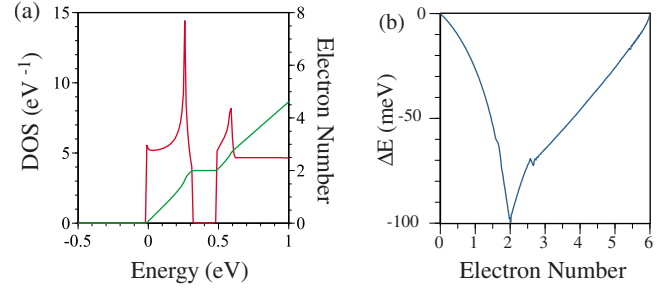


FIG. 3. (Color online) (a) The DOS and filling electron number with respect to energy, calculated for the NFE model in the 2D hexagonal lattice. DOS is colored in red and indicated by the left axis while the electron number in green and by the right axis. (b) Calculated energy difference,  $\Delta E$ , between free electrons and NFE electrons in the hexagonal lattice with number of electron in a unit cell.

$$E_{bs} = \frac{1}{2} \sum_{i \neq j} V(r_{ij}), \quad (3)$$

where  $r_{ij}$  is the interatomic distance and  $V$  presents the Friedel oscillation for large  $r_{ij}$ . In this approach, one expects that the phase is stabilized if the positions of the atoms are such that they tend to be localized in local minima of the interaction  $V(r_{ij})$ . This implies a correlation between the Fermi wavelength (Fermi wave number),  $\lambda_F = 2\pi/k_F$ , and interatomic distances  $r_{ij}$ , implying that the Fermi sphere of the free electron is in contact with a Brillouin zone. Interactions between atoms on surfaces for large  $r_{ij}$  have been well investigated<sup>25,26</sup> and the interaction energy can be expressed with 2D Friedel oscillations,

$$V(r_{ij}) \sim -\xi_F \left[ \frac{2 \sin(\delta_F)}{\pi} \right]^2 \frac{\sin(2k_F r_{ij} - 2\delta_F)}{(k_F r_{ij})^2}, \quad (4)$$

where  $\xi_F (= \frac{\hbar^2 k_F^2}{2m^*})$  and  $\delta_F$  are Fermi energy and the phase shift, respectively. The interaction energy decays with  $1/r_{ij}^2$ , which is in contrast to the  $1/r_{ij}^3$  dependence in the 3D system.<sup>2,3</sup>

For the local atom positions of the  $\sqrt{21} \times \sqrt{21}$  phase for the  $E_{bs}$  calculation, we recall the atomic structure models determined by the experimental structure analyses<sup>5,6,8</sup> and the first-principles calculations.<sup>13,16</sup> As shown in Figs. 4(a) and 4(b), the  $\sqrt{21} \times \sqrt{21}$  superstructure is basically composed of the  $\sqrt{3} \times \sqrt{3}$  structure of the inequivalent trimer (IET) model,<sup>27</sup> prepared by the 1 ML-Ag deposition on the clean Si(111) surface, and three adatoms of (a) alkali metal<sup>6</sup> and (b) noble metal<sup>5,8</sup> in the  $\sqrt{21} \times \sqrt{21}$  unit cell. In the latter case, detailed atom positions have been examined by the theoretical calculation.<sup>13</sup> Since an arrangement of the adatoms on the  $\sqrt{3} \times \sqrt{3}$ -Ag surface structure [large circles in Figs. 4(a) and 4(b)], determines the  $\sqrt{21} \times \sqrt{21}$  periodicity, it indicates that ion pairs between the adatoms are likely sufficient to calculate  $V(r_{ij})$ . The representative interatomic distance at different lengths,  $d_i$  and  $d'_i$ , are shown in Fig. 4 for the noble-metal model and the alkali-metal models, respectively. It is noted that alkali-metal adatoms keep the same distance between each other while three noble metal adatoms gather. Through a summation over all the  $V(d_i)$  or  $V(d'_i)$

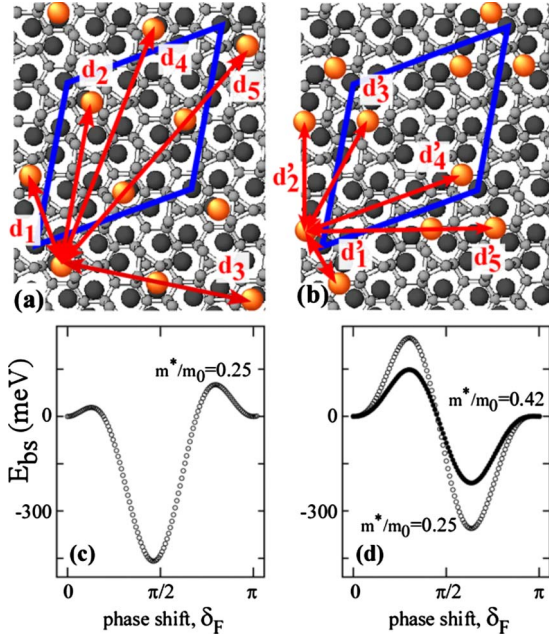


FIG. 4. (Color online) (a) and (b) Schematic drawing of the  $\sqrt{21} \times \sqrt{21}$  surface structure models: adatoms (large orange circles) of the (a) alkali metal and (b) noble metal on the  $\sqrt{3} \times \sqrt{3}$  IET model (Refs. 5, 6, and 8). Representative interatomic distance up to the fifth nearest neighbors,  $d_1-d_5$  and  $d'_1-d'_5$ , are indicated with (red) arrows in (a) and (b). The  $\sqrt{21} \times \sqrt{21}$  unit cell is shown by blue lines. (c) and (d) Band structure energy,  $E_{bs}$ , per unit cell calculated as a function of the phase shift,  $\delta_F$ , in a case of three electrons in the unit cell.

values for the equivalent sites,  $E_{bs}$  for the two structure models, Figs. 4(a) and 4(b), can be calculated. The interatomic distance was chosen up to the 11th nearest neighbors, being enough for negligible size dependence of  $E_{bs}$  compared to the energy differences with the electron number. The  $m^*$  values in the  $V(r_{ij})$  calculation were chosen from bottom of the parabolic band dispersion at  $\bar{\Gamma}$ ,  $m^*/m_0=0.42$  in Fig. 2 and  $m^*/m_0=0.25$  from the previous photoemission experiment.<sup>4</sup>

The  $\delta_F$  values in  $V(r_{ij})$  were determined by the minimum  $E_{bs}$  energy at 3 electrons/cell. In a framework of the perturbation calculation, the  $k_F$  in Eq. (4) is given from the unperturbed free-electron term and the relation, Eq. (2), was used ( $k_F=0.265 \text{ \AA}^{-1}$ ). Figures 4(c) and 4(d) show results on  $E_{bs}$  energy changes with  $\delta_F$ . The minimum was found at  $\delta_F^a=0.49\pi$  for (a) the alkali metal while at  $\delta_F^b=0.67\pi$  for (b) the noble-metal models. Theoretically,  $\delta_F$  corresponds to the scattering phase shift of an electron standing wave around an atom<sup>25</sup> and it can also be obtained from the observations by scanning tunneling spectroscopy.<sup>19,25,28-30</sup> The experimental phase shift<sup>26</sup> for a Cs atom on Cu(111) was  $(0.43 \pm 0.08)\pi$ , which is the same as  $\delta_F^a$  within the error. The value is consistent to  $\delta_F^a=0.5\pi$  according to the Friedel's sum rule by assuming a positively charged (+1) scatterer with  $s$ -orbital symmetry.<sup>28</sup> On the other hand,  $\delta_F^b$  is deviated from the simple argument, requiring the experimental confirmation. Figure 5 exhibits results of STM/STS observations around a 2D nanocluster, which is a precursor of the  $\sqrt{21} \times \sqrt{21}$  phase.<sup>5,20</sup> Tip bias around  $-1 \text{ V}$  was chosen to compensate

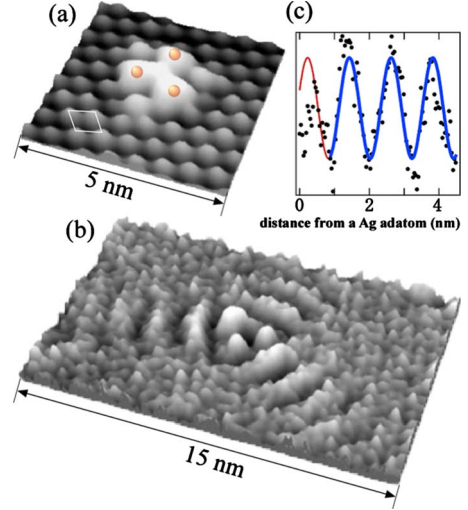


FIG. 5. (Color online) (a) An STM image of a 2D nanocluster or a precursor of the  $\sqrt{21} \times \sqrt{21}$  phase (Refs. 5 and 20) The three Ag atoms, forming the 2D nanocluster are depicted as three orange spheres. The  $\sqrt{3} \times \sqrt{3}$  unit cell is shown with white lines. (b) An STS image of standing waves around the 2D nanocluster. (c) A line profile of one of the standing waves. The blue thick curve is the fitted sinusoidal function and the red thin curve is extrapolation to the adatom position. All the images in the figure were taken at 5 K with tip bias of  $-1 \text{ V}$  (Refs. 19 and 31).

the tip-induced band-bending effect<sup>31</sup> and to probe standing waves of wavelengths at  $\lambda=2\pi/2k_F$ . The 2D nanocluster is composed of three Ag atoms, forming a threefold propeller structure in an STM image in Fig. 5(a). The STS image in Fig. 5(b) gives clear standing waves toward the three symmetric direction from the three atoms. Figure 5(c) is a line profile of one of the standing waves and, from a curve fitting of the wave with a sinusoidal function, the phase shift at the Ag atom was determined as  $\delta_F^{Ag}=(0.63 \pm 0.05)\pi$ . The value matches to the result of the  $E_{bs}$  calculation in Fig. 4(d). It is noted the previous STM/STS report<sup>29</sup> have found that a single adatom on Si(111) $\sqrt{3} \times \sqrt{3}$ -Ag had the phase shift of  $\delta_F^{Ag}=-0.34\pi$ . Since the  $V(r_{ij})$  function has the modulo of  $\pi$ ,  $\delta_F^{Ag}$  equals to  $0.66\pi$ , which also matches to  $\delta_F^b$ . Using these appropriate  $\delta_F^a$  and  $\delta_F^b$  values,  $E_{bs}$  is calculated at different numbers of electrons in the  $\sqrt{21} \times \sqrt{21}$  unit cell, corresponding to the different Fermi wave number ( $k_F$ ) in  $V(r_{ij})$ . A summary of  $E_{bs}$  are shown in Fig. 6 as a function of a number of electrons in the unit cell.  $E_{bs}$  for the structure models of both alkali metal, Fig. 4(a), and noble metal, Fig. 4(b), reach the minimum at three electrons in the unit cell. These results explain the stability of the  $\sqrt{21} \times \sqrt{21}$  phase at three electrons, rather than at two electrons, irrespective of the surface atomic structure models and the  $m^*$  values. Despite the simple calculation, the conclusion of the present pseudopotential approach match to the experimental findings, listed in Table I.

As described above, the pseudopotential approach with  $E_{bs}$  successfully describes the constant  $e/a$  ratio, the 2D electron compound nature, of the  $\sqrt{21} \times \sqrt{21}$  phase. Here, we further discuss  $\delta_F^a$  and  $\delta_F^b$  in the ion-pair interaction. The scattering phase shift,  $\delta_F$ , depends on a potential at a scat-

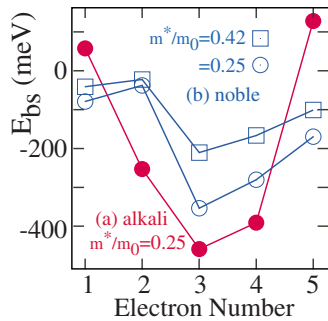


FIG. 6. (Color online) Calculated band-structure energy,  $E_{bs}$ , per unit cell with different numbers of electrons in a unit cell. The blue open circles and squares are results of Fig. 4(b) while the red solid circles are those of Fig. 4(a). In the calculation, ion pairs were chosen up to the 11th nearest neighbors.

terer and it varies with (pseudo)potentials of elements. Thus, the difference in the  $\delta_F^a$  and  $\delta_F^b$  values is mainly due to distinction between the alkali- and noble-metal atoms. Since the alkali and noble metal adatoms are monovalent on the surface,<sup>4,14,15</sup> this naturally explains  $\delta_F^a \approx \delta_F^b$  and that the deviation from  $\delta_F^a$  for  $\delta_F^b$  may be due to existence of inner  $d$ -orbital for noble metals. It is intriguing to note that the difference of atomic structure of Figs. 4(a) and 4(b) can be explained by the slight difference of the phase shift,  $\delta_F^a - \delta_F^b = -0.18\pi$ , in the present pseudopotential model. Further quantitative analyses with the 2D partial wave expansions<sup>28</sup>

of  $s$ ,  $p$ ,  $d$  waves<sup>32,33</sup> of each element or the three-adsorbate interaction corrections<sup>34</sup> may explain the whole picture of the surface-state-mediated interactions in the  $\sqrt{21} \times \sqrt{21}$  phase.

#### IV. CONCLUSION

In summary, the  $\sqrt{21} \times \sqrt{21}$  phase, prepared by coadsorption of monovalent atoms on Si(111), was found to possess electron compound nature. Using this 2D metal alloys phase, two competing theories conventionally applied for the Hume-Rothery compounds, Jones model, and pseudopotential model, were examined. Only the pseudopotential approach matched to the experimental results. The present research indicates that the simple analytical approach with medium-range interaction enables to argue stability of the surface superstructures of metal alloys.

#### ACKNOWLEDGMENTS

Uichiro Muzutani, Ken-ichi Tanaka, and Ayahiko Ichimiya are gratefully acknowledged for valuable comments and discussions. Ryu Yukawa is appreciated for supporting the theoretical simulation. W.H.C. and H.W.Y. are supported by CRI program of MEST, Korea. This work was supported by Grants-In-Aid from Japan Society for the Promotion of Science and was a part of the A3 Foresight Program funded by JSPS-KOSEF-NSFC. The supporting experiments have been also done at BL-18A, KEK-PF, Japan.

\*imatsuda@issp.u-tokyo.ac.jp

<sup>1</sup>C. Kittel, *Introduction to Solid State Physics* (Wiley, New York, 1995), Chap. 21.

<sup>2</sup>T. B. Massalski and U. Mizutani, *Prog. Mater. Sci.* **22**, 151 (1978).

<sup>3</sup>G. T. de Laissardière, D. Nguyen-Manh, and D. Mayou, *Prog. Mater. Sci.* **50**, 679 (2005).

<sup>4</sup>I. Matsuda, T. Hirahara, M. Konishi, C. Liu, H. Morikawa, M. D'angelo, S. Hasegawa, T. Okuda, and T. Kinoshita, *Phys. Rev. B* **71**, 235315 (2005).

<sup>5</sup>C. Liu, I. Matsuda, M. D'angelo, S. Hasegawa, J. Okabayashi, S. Toyoda, and M. Oshima, *Phys. Rev. B* **74**, 235420 (2006).

<sup>6</sup>C. Liu, S. Yamazaki, R. Hobarra, I. Matsuda, and S. Hasegawa, *Phys. Rev. B* **71**, 041310(R) (2005).

<sup>7</sup>M. D'angelo, M. Konishi, I. Matsuda, C. Liu, S. Hasegawa, T. Okuda, and T. Kinoshita, *Surf. Sci.* **590**, 162 (2005).

<sup>8</sup>Y. Fukaya, A. Kawasuso, and A. Ichimiya, *Surf. Sci.* **600**, 3141 (2006).

<sup>9</sup>A. Ichimiya, H. Nomura, Y. Horio, T. Sato, T. Sueyoshi, and M. Iwatsuki, *Surf. Rev. Lett.* **1**, 1 (1994).

<sup>10</sup>Y. L. Gavriljuk, V. G. Lifshits, and N. Enebish, *Surf. Sci.* **297**, 345 (1993).

<sup>11</sup>J. Yuhara, R. Ishigami, and K. Morita, *Surf. Sci.* **326**, 133 (1995).

<sup>12</sup>J. Yuhara, M. Inoue, and K. Morita, *J. Vac. Sci. Technol. A* **11**, 2714 (1993).

<sup>13</sup>H. Jeong, H. W. Yeom, and S. Jeong, *Phys. Rev. B* **77**, 235425

(2008).

<sup>14</sup>H. M. Zhang, K. Sakamoto, and R. I. G. Uhrberg, *Phys. Rev. B* **64**, 245421 (2001); **70**, 245301 (2004).

<sup>15</sup>J. N. Crain, K. N. Altmann, C. Bromberger, and F. J. Himpsel, *Phys. Rev. B* **66**, 205302 (2002).

<sup>16</sup>X. Xie, J. M. Li, W. G. Chen, F. Wang, S. F. Li, Q. Sun, and Yu Jia, *J. Phys.: Condens. Matter* **22**, 085001 (2010).

<sup>17</sup>I. Matsuda, M. Hengsberger, F. Baumberger, T. Greber, H. W. Yeom, and J. Osterwalder, *Phys. Rev. B* **68**, 195319 (2003).

<sup>18</sup>W. H. Choi, P. G. Kang, K. D. Ryang, and H. W. Yeom, *Phys. Rev. Lett.* **100**, 126801 (2008).

<sup>19</sup>M. Ono, Y. Nishigata, T. Nishio, T. Eguchi, and Y. Hasegawa, *Phys. Rev. Lett.* **96**, 016801 (2006).

<sup>20</sup>N. Sato, T. Nagao, and S. Hasegawa, *Phys. Rev. B* **60**, 16083 (1999).

<sup>21</sup>J. Nogami, K. J. Wan, and X. F. Lin, *Surf. Sci.* **306**, 81 (1994).

<sup>22</sup>Y. Fukaya, I. Matsuda, M. Hashimoto, H. Narita, A. Kawasuso, and A. Ichimiya, *e-J. Surf. Sci. Nanotechnol.* **7**, 432 (2009).

<sup>23</sup>A. Kawasuso and S. Okada, *Phys. Rev. Lett.* **81**, 2695 (1998).

<sup>24</sup>K. Hayashi, A. Kawasuso, and A. Ichimiya, *Surf. Sci.* **600**, 4426 (2006).

<sup>25</sup>P. Hyldgaard and M. Persson, *J. Phys.: Condens. Matter* **12**, L13 (2000).

<sup>26</sup>Th. von Hofe, J. Kröger, and R. Berndt, *Phys. Rev. B* **73**, 245434 (2006).

<sup>27</sup>I. Matsuda and S. Hasegawa, *J. Phys.: Condens. Matter* **19**,

- 355007 (2007).
- <sup>28</sup>P. Avouris, I.-W. Lyo, R. E. Walkup, and Y. Hasegawa, *J. Vac. Sci. Technol. B* **12**, 1447 (1994).
- <sup>29</sup>S. Minamoto, Y. Ogawa, Y. Sano, and H. Hirayama, *Physica E* **40**, 324 (2007).
- <sup>30</sup>I. Matsuda, M. Ueno, T. Hirahara, R. Hobara, H. Morikawa, C. Liu, and S. Hasegawa, *Phys. Rev. Lett.* **93**, 236801 (2004).
- <sup>31</sup>T. Hirahara, I. Matsuda, M. Ueno, and S. Hasegawa, *Surf. Sci.* **563**, 191 (2004).
- <sup>32</sup>W. H. Young, A. Meyer, and G. E. Kilby, *Phys. Rev.* **160**, 482 (1967).
- <sup>33</sup>J. M. Dickey, A. Meyer, and W. H. Young, *Phys. Rev.* **160**, 490 (1967).
- <sup>34</sup>P. Hyldgaard and T. L. Einstein, *Europhys. Lett.* **59**, 265 (2002).